# MEASUREMENTS OF ATMOSPHERIC NEUTRINOS IN THE SUPER–KAMIOKANDE DETECTOR

**Masato Shiozawa** *

*On behalf of*

the Super–Kamiokande Collaboration

*Kamioka Observatory, ICRR, Univ. of Tokyo*

*Higashi-mozumi, Kamioka-cho, Yoshiki-gun, Gifu 506-1205, JAPAN*

**Abstract**

We have measured atmospheric neutrinos using data from a 25.5 kton·year of the Super–Kamiokande detector. Using detailed flux calculations and detector simulations, we confirm that the flavor ratio $\nu_\mu/\nu_e$ is significantly smaller than the expected value. Measured zenith angle distributions indicate that the small flavor ratio is due to a deficit of upward going muon neutrinos. The neutrino oscillation hypothesis is strongly supported by the observed zenith angle distributions as well as the anomalous flavor ratio.

*E-mail: masato@icrkm4.icrr.u-tokyo.ac.jp

# 1 Introduction

The Super–Kamiokande experiment has started its operation on April 1st, 1996 and we already have roughly two years of data for physics analyses. The experiment can investigate several physics topics: a proton decay search, measurements of atmospheric neutrinos, and solar neutrinos [1]. The first results are ready for each of these analyses and several results have been already submitted [2, 3, 4, 5].

One of the major goals of the Super–Kamiokande experiment is measurement of the atmospheric neutrinos. Atmospheric neutrinos were originally studied as background for proton decay searches because neutrino interactions in the detector could mimic a proton decay signal. The detailed study brought recognition of the anomalous flavor ratio and also its baseline dependence [6]. These results suggested that neutrino flavor oscillations were taking place between the neutrino production points and the detectors. However, some experiments reported a flavor ratio consistent with expectations. Therefore the situation was somewhat controversial and more data were needed.

# 2 Atmospheric Neutrinos

Atmospheric neutrinos are decay products of secondary particles which are produced in hadronic showers caused by primary cosmic rays high in the atmosphere. The neutrinos are mainly produced via the decay chains of pions as following: $\pi^+ \to \mu^+ + \nu_\mu$; the muon decays as $\mu^+ \to e^+ + \overline{\nu}_\mu + \nu_e$ (and charge conjugates). Therefore, the neutrino flavor ratio $(\nu_\mu + \overline{\nu}_\mu)/(\nu_e + \overline{\nu}_e)$ $(\equiv \nu_\mu/\nu_e)$ is about two in the low energy region ($< 1$ GeV) where almost all muons decay before reaching the Earth. In higher energy region, however, the decays of the muons in flight are supressed and the flavor ratio increases. While the absolute flux of the neutrinos has a large uncertainty ($\sim 20\%$), the flavor ratio $\nu_\mu/\nu_e$ has $< 5\%$ uncertainty.

The atmospheric neutrino flux is calculated by several authors (see, for example [7, 8]) taking into account the measured flux of primary cosmic rays, geomagnetic cutoff effect, productions of secondary particles, and their decays. Several different calculations are compared by the authors themselves and they cannot find anything with a strong effect on the predicted $\nu_\mu/\nu_e$ ratio [9].

Atmospheric neutrino experiments observe electrons and muons from neutrino interactions in the detector and compare these observations with the expected ones. By taking the ratio of the number of muon events to electron events $(\equiv \mu/e)$, the uncertainties of neutrino cross sections as well as the absolute flux uncertainty are largely cancelled out. The several measured $\mu/e$ ratios divided by the expected ones, namely the double ratio $(\mu/e)_{DATA}/(\mu/e)_{MC} (\equiv R)$ are listed in Table 1. Two water Cherenkov detector experiments, Kamiokande (sub-GeV and multi-GeV region) and IMB (sub-GeV), measured small double ratios of $\sim 0.6$ with relatively high statistics. Kamiokande also observed the zenith angle dependence of the double ratio. Soudan-2, an iron calorimeter experiment, also reported an anomalous double ratio which is consistent with the Kamiokande and IMB sub-GeV results. However, the results from other iron calorimeter experiments, Fréjus and NUSEX, and IMB in the multi-GeV region, are consistent with expectations. The Super–Kamiokande experiment can measure the double ratio and its

| | | $R \equiv (\mu/e)_{DATA}/(\mu/e)_{MC}$ | Exposure (kton·year) |
|---|---|---|---|
| Kamiokande [6, 10] | (sub-GeV) | $0.60^{+0.06}_{-0.05} \pm 0.05$ | 7.7 |
| | (multi-GeV) | $0.57^{+0.08}_{-0.07} \pm 0.07$ | 6.0 – 8.2 |
| IMB [11] | (sub-GeV) | $0.54 \pm 0.05 \pm 0.12$ | 7.7 |
| | | $1.40^{+0.41}_{-0.30} \pm 0.3$ | 2.1 |
| Fréjus [12] | | $1.00 \pm 0.15 \pm 0.08$ | 1.56 |
| NUSEX [13] | | $0.96^{+0.32}_{-0.28}$ | 0.7 |
| Soudan–2 [14] | | $0.61 \pm 0.15 \pm 0.05$ | 3.2 |

Table 1: Summary of the measured double ratios.

zenith angle dependence with much higher statistics than ever before. This experiment is expected to resolve the atmospheric neutrino anomaly.

If the anomalous double ratios are due to neutrino oscillations, one might observe energy and/or path length dependence of R. If mass eigenstates of $\nu_1$ and $\nu_2$ have nonzero neutrino masses $m_1$ and $m_2$, the flavor eigenstates of neutrinos ($\nu_l$, $\nu_{l'}$) are related to the mass eigenstates as:

$$\begin{pmatrix} \nu_l \\ \nu_{l'} \end{pmatrix} = \begin{pmatrix} \cos\theta & \sin\theta \\ -\sin\theta & \cos\theta \end{pmatrix} \begin{pmatrix} \nu_1 \\ \nu_2 \end{pmatrix} \tag{1}$$

Only two neutrino generations are considered here for simplicity. $\theta$ is the mixing angle between the two mass eigenstates. The survival probability for $\nu_l \to \nu_l$ is given by:

$$P(\nu_l \to \nu_l) = \sin^2 2\theta \sin^2(1.27 \frac{\Delta m^2[\mathrm{eV}^2] L[\mathrm{km}]}{E[\mathrm{GeV}]}) \tag{2}$$

where $E$ and $L$ are the energy and the path length of the neutrinos, and $\Delta m^2 = |m_2^2 - m_1^2|$.

In experiments, the energy and direction of the final state leptons represent the neutrino energy $E$ and the path length $L$. Atmospheric neutrinos in the 0.1 $\sim$ 10 GeV energy range are relevant to observations of contained events. Since the experiments are performed near the surface of the Earth, we observe neutrinos with path lengths of 10 km (down-going neutrinos) up to 13000 km (up-going neutrinos). The angular correlations between the initial neutrinos and the final state leptons are crucial for the neutrino oscillation analysis; the correlation for $\nu_\mu - \mu$ in quasi-elastic scattering is $> 70^\circ$ for lepton momentum $p_\mu < 400$ MeV/$c$, and improves to $\sim 25^\circ$ for $p_\mu = 1$ GeV/$c$ and $< 15^\circ$ for $p_\mu > 2$ GeV/$c$.

# 3 Super–Kamiokande detector

Super–Kamiokande is a large water Cherenkov detector located in the Mozumi mine at 2700 meters-water-equivalent below the peak of Mt. Ikenoyama in Kamioka, Gifu prefecture, Japan. The detector holds 50 ktons of ultra-pure water contained in a cylindrical stainless steel tank measuring 41.4 m in height and 39.3 m in diameter. The water is optically separated into two concentric cylindrical regions.

The inner detector is 36.2 m high and 33.8 m in diameter and viewed by 11146, inward-facing, 50 cm diameter photomultiplier tubes (PMTs). These PMTs uniformly surround the region giving a photocathode coverage of 40%. An ADC/TDC system records the number and arrival times of the Cherenkov photons collected in each PMT. From these values, along with the positions of the PMTs, the events are reconstructed. The 2.5–2.7 m thick outer detector completely surrounds the inner detector. This region is viewed by 1885 outward pointing 20 cm diameter PMTs. The primary function of the outer detector is to veto cosmic ray muons and to help identify contained events.

The trigger we use in this analysis is issued when 29 or more inner PMTs produce signals greater than 1/4 p.e. in a 200 ns coincidence window. This trigger threshold corresponds to the mean number of PMTs hit by the Cherenkov photons from a 5.7 MeV electron. The trigger rate ranges between 10 Hz and 12 Hz, of which 2.2 Hz is due to cosmic ray muons entering the inner detector.

# 4 Results

We show the results of atmospheric neutrino observations in 414 live-days of data between May 1996 and October 1997, corresponding to an exposure of 25.5 kton·year in Super–Kamiokande. Starting from about 400 million events, the contained events were extracted by applying a reduction algorithm to reject low energy radioactivity backgrounds and entering cosmic ray muons. We classify contained events as fully contained (FC) events in which all energy is deposited in the inner detector, and partially contained (PC) events in which one of visible tracks exits the inner detector into the outer detector. For both types of event, the neutrino interaction points are required to be inside the fiducial volume, 2 m inside the inner detector PMT plane. For this analysis, single-ring FC events and PC events are used. Each single-ring FC event is classified as an $e$-like event or a $\mu$-like event, using the photon distribution of its Cherenkov ring. All PC events are classified as $\mu$-like events.

## 4.1 Flavor Ratio

Table 2 summarizes the observed FC and PC events along with Monte Carlo (MC) predictions. We use the flux calculations of [7]. For the sub-GeV sample, we require $p_e > 100$ MeV/$c$ for $e$-like events and $p_\mu > 200$ MeV/$c$ for $\mu$-like events, and visible energy $< 1.33$ GeV. The FC events with visible energy $> 1.33$ GeV and all PC events comprise the multi-GeV sample.

For these observed events, the double ratio for the sub-GeV sample is:

$$\frac{(\mu/e)_{DATA}}{(\mu/e)_{MC}} = 0.610\ ^{+0.029}_{-0.028}\ (\text{stat.}) \pm 0.049\ (\text{sys.}) \qquad (\text{sub-GeV})$$

Combining multi-GeV FC events and PC events, the double ratio for the multi-GeV sample is:

$$\frac{(\mu/e)_{DATA}}{(\mu/e)_{MC}} = 0.659\ ^{+0.058}_{-0.053}\ (\text{stat.}) \pm 0.08\ (\text{sys.}) \qquad (\text{multi-GeV})$$

| | | DATA | MC | $\nu_e, \overline{\nu}_e$ CC | $\nu_\mu, \overline{\nu}_\mu$ CC | NC |
|---|---|---|---|---|---|---|
| sub-GeV | FC e-like | 983 | 812.2 | 88% | 2% | 10% |
| | FC $\mu$-like | 900 | 1218.3 | 0.5% | 96% | 4% |
| multi-GeV | FC e-like | 218 | 182.7 | 84% | 7% | 9% |
| | FC $\mu$-like | 176 | 229.0 | 0.6% | 99% | 0.4% |
| | PC ($\mu$-like) | 230 | 287.7 | 1.5% | 98% | 0.7% |

Table 2: Summary of observed events and MC predictions. The estimated contributions from charged current (CC) interactions and neutral current (NC) interactions are also shown.

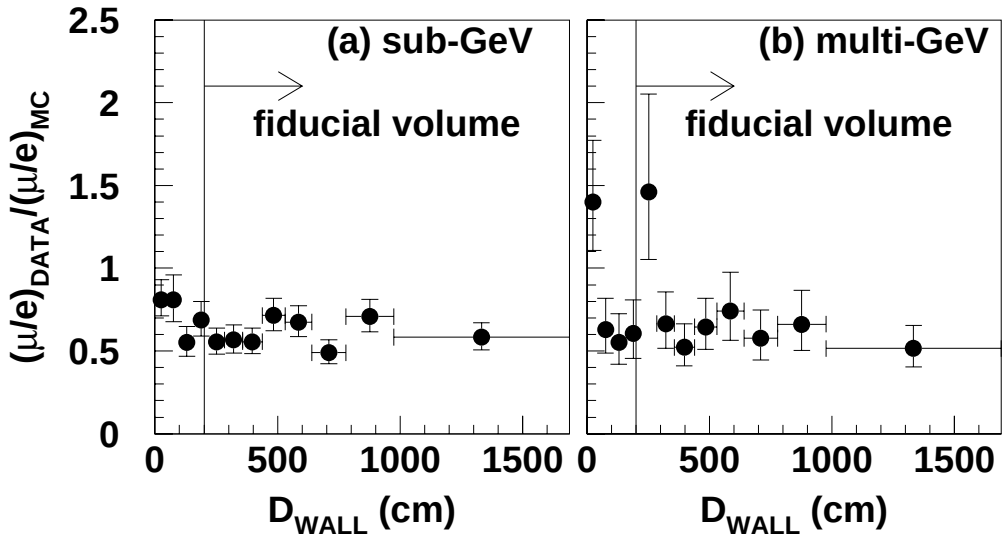


Figure 1: The double ratio as a function of $D_{WALL}$, the distance between the event vertex and the nearest inner detector wall, for (a) sub-GeV and (b) multi-GeV sample. The region $D_{WALL} > 2$ m is the fiducial volume.

The uncertainties of the $\nu_\mu/\nu_e$ flux calculations (5%) and the neutrino cross sections (4.6% for sub-GeV and 5.9% for multi-GeV) are included in the systematic errors, as well as experimental errors. Therefore, these double ratios are significantly smaller than expectations and consistent with the results of Kamiokande. Figure 1 shows the $D_{WALL}$ dependence of the double ratio where $D_{WALL}$ is the distance between the event vertex and the nearest inner detector wall. The double ratio has no significant dependence on $D_{WALL}$ for either the sub-GeV or the multi-GeV range.

## 4.2 Energy Dependence

The momentum distributions for $e$-like events, $\mu$-like events, and the double ratio are shown in Figure 2. Although the numbers of $e$-like events and $\mu$-like events disagree with expectations, the shapes of the momentum distributions are similar to those of the Monte Carlo distributions for both sub-GeV and multi-GeV samples. No significant energy dependence of R is observed.

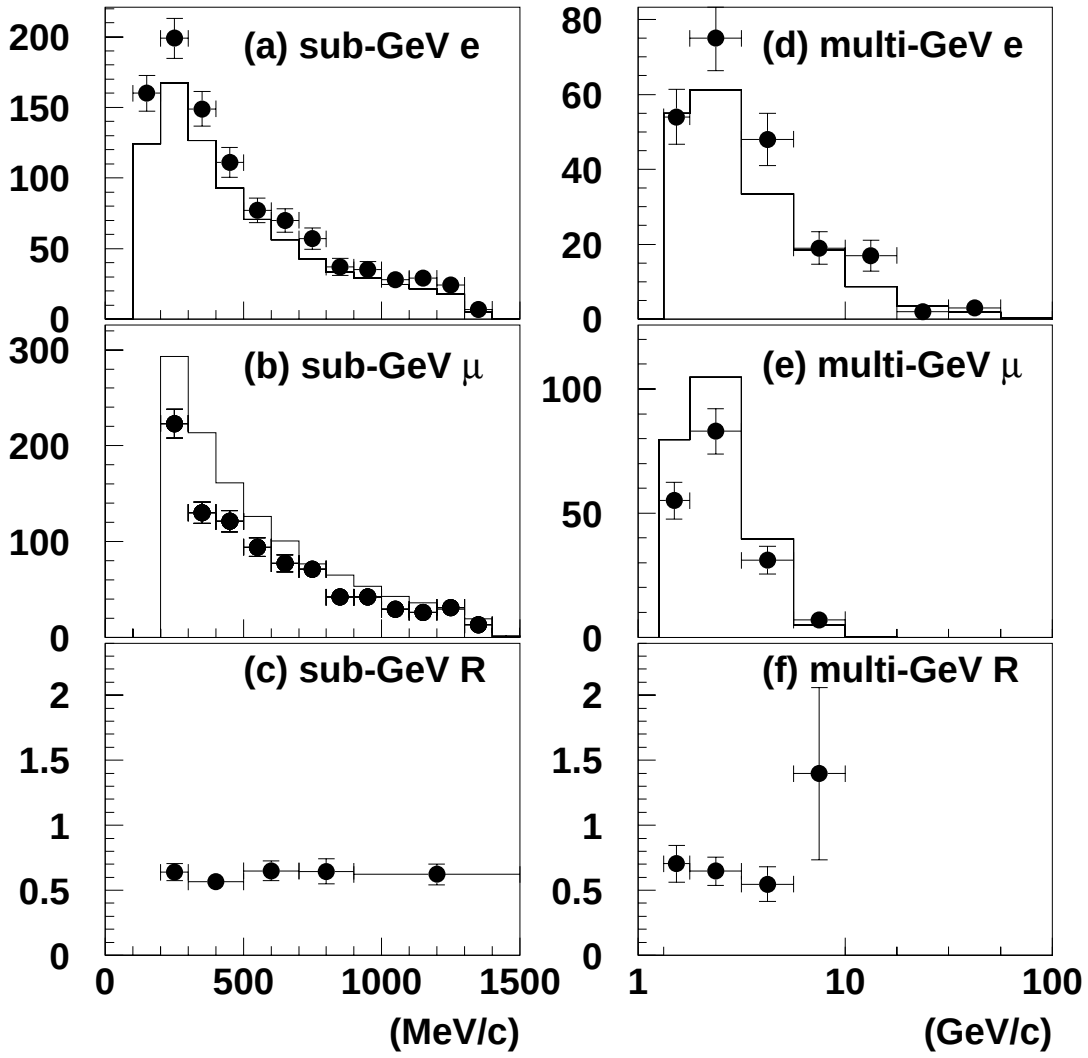


Figure 2: The momentum distributions for (a) sub-GeV $e$-like, (b) sub-GeV $\mu$-like, (c) sub-GeV double ratio, (d) multi-GeV $e$-like, (e) multi-GeV $\mu$-like, and (f) multi-GeV double ratio. The histograms show the Monte Carlo predictions. Error bars represent statistical errors only.

| Monte Carlo Fit Parameters | Uncertainty | Best Fit |
|---|---|---|
| $\nu$ flux normalization | 20% | 16.5% |
| $\nu$ flux spectral index | 0.05 | 0.0058 |
| sub-GeV $\mu/e$ ratio | 8% | -8.6% |
| multi-GeV $\mu/e$ ratio | 12% | -5.9% |
| relative norm. of PC to FC | 8% | 2.8% |

Table 3: Summary of Monte Carlo fit parameters. Best fit values for $\nu_\mu \leftrightarrow \nu_\tau$ and estimated uncertainties are given. All parameters are introduced so as to have zero expectation value.

## 4.3 Zenith Angle Dependence

To investigate the path length dependence of the neutrino flux, each zenith angle $\cos\theta_z$ of the final lepton direction is filled into five bins. Figure 3 shows the zenith angle distributions for (a) sub-GeV $e$-like, (b) sub-GeV $\mu$-like, (c) multi-GeV $e$-like, and (d) multi-GeV $\mu$-like events. The shape of the data (circles) and Monte Carlo (shaded histograms) distributions agree with each other for the sub-GeV and multi-GeV $e$-like samples but not for the $\mu$-like samples. In particular, there is a large deficit of up-going $\mu$-like events in the multi-GeV region. For this sample, the up/down ratio, defining up-going events as those with $-1 < \cos\theta_z < -0.2$ and down-going events as those with $0.2 < \cos\theta_z < 1$, is up/down $= 0.52^{+0.07}_{-0.06}$, $5.7\sigma$ deviation from unity. The systematic uncertainty for the up/down ratio of multi-GeV $\mu$-like events is only 3%, comprising 1.5% from flux calculations, 2% from a contamination of cosmic ray muons, and 1.5% from energy calibration.

## 4.4 Oscillation Analysis

Since the zenith angle distributions for $e$-like events agree with those of Monte Carlo, the data favor $\nu_\mu \leftrightarrow \nu_\tau$ oscillations rather than $\nu_e \leftrightarrow \nu_\mu$ oscillations. We perform a detailed statistical fit of a two flavor $\nu_\mu \leftrightarrow \nu_\tau$ oscillation hypothesis to the data taking into account the systematic uncertainties. All important Monte Carlo parameters are allowed to vary weighted by their systematic uncertainties. The systematic uncertainties are listed in Table 3 along with each of the best fit values for our data. The contour plots in two dimensional parameter space of $\sin^2 2\theta$ and $\Delta m^2$ are shown in Figure 4. Large mixing angle in the range $\sin^2 2\theta > 0.7$ and $\Delta m^2$ in the range $3 \times 10^{-4}$ eV$^2$ $< \Delta m^2 < 9 \times 10^{-3}$ eV$^2$ are allowed at 99% confidence level. Using one typical point $(\sin^2 2\theta, \Delta m^2) = (1.0, 5 \times 10^{-3}\text{eV}^2)$ in the allowed region, zenith angle distributions for the fitted Monte Carlo are overlaid in Figure 3. The data are well reproduced by the fitted Monte Carlo. Therefore, the large distortion in the zenith angle distributions can be interpreted as path length dependence of neutrino oscillations.

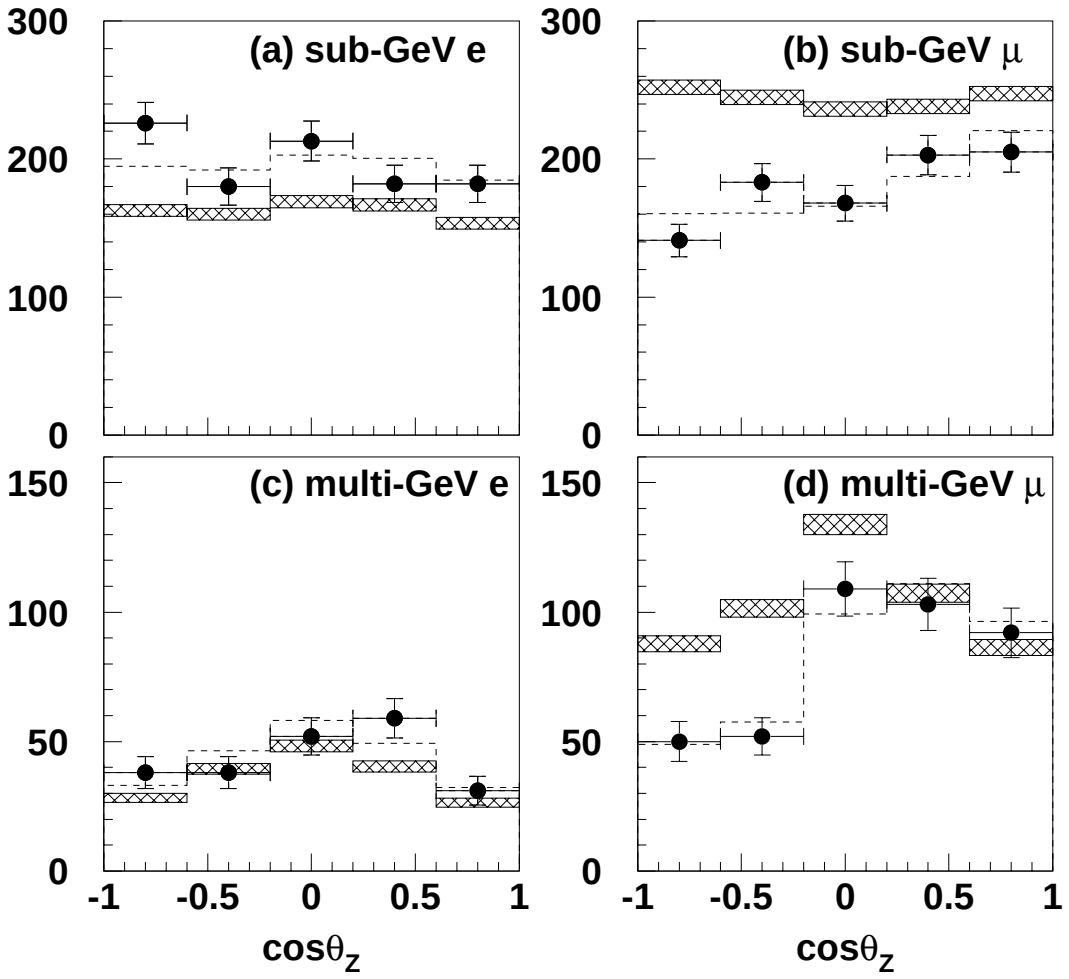


Figure 3: The zenith angle distributions for (a) sub-GeV $e$-like, (b) sub-GeV $\mu$-like, (c) multi-GeV $e$-like, and (d) multi-GeV $\mu$-like events. The data (circles) and Monte Carlo (shaded histograms) with statistical errors are shown. Up-going and down-going correspond to $\cos\theta_z = -1$ and $\cos\theta_z = 1$, respectively. The dotted line shows the fitted Monte Carlo with a $\nu_\mu \leftrightarrow \nu_\tau$ oscillation hypothesis with $(\sin^2 2\theta, \Delta m^2) = (1.0, 5 \times 10^{-3}\mathrm{eV}^2)$.

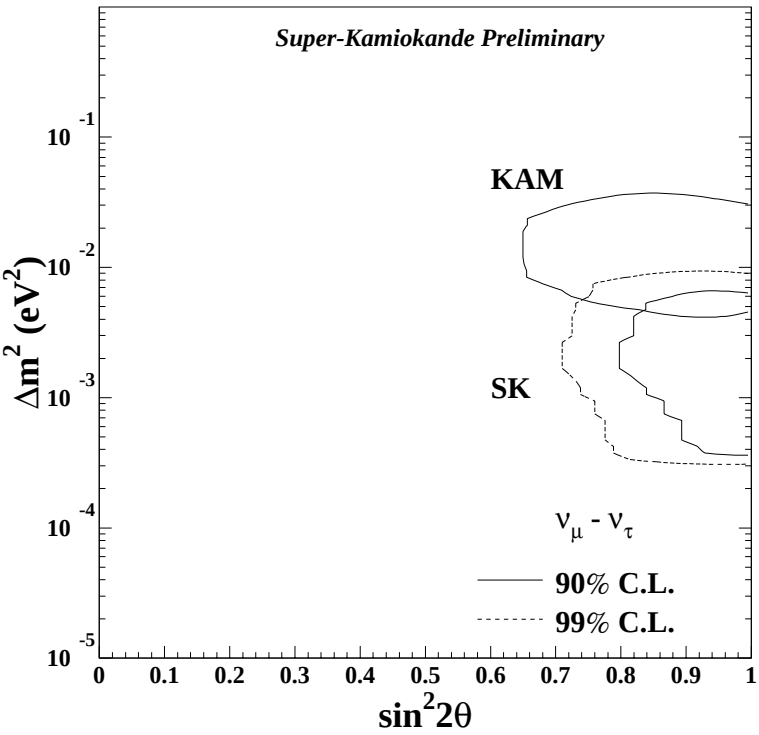


Figure 4: The 90% and 99% confidence intervals for $\nu_\mu \leftrightarrow \nu_\tau$ two flavor oscillations. The Kamiokande result (KAM) is also shown along with the Super–Kamiokande results (SK).

# 5 Conclusion

The Super–Kamiokande experiment has been in operation since April 1996 and several physics topics are being addressed. Among these topics, measurements of atmospheric neutrinos give very impressive results. With high statistics, we confirm an anomalous double ratio $(\mu/e)_{DATA}/(\mu/e)_{MC}$ which is consistent with Kamiokande's result. The zenith angle distributions indicate that the anomaly is due to a large deficit of up-going $\mu$-like events. A $\nu_\mu \leftrightarrow \nu_\tau$ two flavor oscillation hypothesis are strongly supported by the event zenith angle distributions and oscillation parameters in the ranges $\sin^2 2\theta > 0.7$ and $3 \times 10^{-4}$ eV$^2$ $< \Delta m^2 < 9 \times 10^{-3}$ eV$^2$ are allowed at 99% confidence level.

# 6 Acknowledgements

The author thanks the conference organizers and the participants for the exciting conference at the fantastic place. He also appreciates the Super–Kamiokande collaborators for much help in preparing the latest results and his talk. He also acknowledges the cooperation of the Kamioka Mining and Smelting Company. The Super–Kamiokande experiment was built from, and has been operated with, funding by the Japanese Ministry of Education, Science, Sports and Culture, and the United States Department of Energy.

[1] M. Takita, *Frontiers of Neutrino Astrophysics ( Proc. of the Int. Symp. on Neutrino Astrophysics,* Takayama, 1992 ), edited by Y. Suzuki and K. Nakamura ( Universal Academy Press, Tokyo, 1993 ) , p.135

[2] Super-Kamiokande collaboration, M. Shiozawa *et al.*, *Search for Proton Decay via* $p \to e^+\pi^0$ *in a Water Cherenkov Detector*, submitted to Phys. Rev. Lett..

[3] Super-Kamiokande collaboration, Y. Fukuda *et al.*, *Measurement of a small atmospheric* $\nu_\mu/\nu_e$ *ratio*, Phys. Lett. **B** (to be published).

[4] Super-Kamiokande collaboration, Y. Fukuda *et al.*, *Study of the atmospheric neutrino flux in the multi-GeV energy range*, submitted to Phys. Lett. **B**.

[5] Super-Kamiokande collaboration, Y. Fukuda *et al.*, *Measurements of the Solar Neutrino Flux from Super–Kamiokande's First 300 Days*, submitted to Phys. Rev. Lett..

[6] Y. Fukuda *et al.*, Phys. Lett. **B335**, 237 (1994).

[7] M. Honda *et al.*, Phys. Rev. **D52**, 4985 (1995).; M. Honda *et al.*, Phys. Lett. **B248**, 193 (1990).

[8] G. Barr *et al.*, Phys. Rev. **D39**, 3532 (1989).; V. Agrawal *et al.*, Phys. Rev. **D53**, 1314 (1996).; T. K. Gaisser and T. Stanev, Proc. 24th Int. Cosmic Ray Conf. (Rome) Vol.1, 694 (1995).

[9] T. K. Gaisser *et al.*, Phys. Rev. **D54**, 5578 (1996).

[10] K. S. Hirata *et al.*, Phys. Lett. **B205**, 416 (1988); K. S. Hirata *et al.*, Phys. Lett. **B280**, 146 (1992).

[11] D. Casper *et al.*, Phys. Rev. Lett. **66**, 2561 (1991); R. Becker-Szendy *et al.*, Phys. Rev. **D46**, 3720 (1992); R. Clark *et al.*, Phys. Rev. Lett. **79**, 345 (1997).

[12] K. Daum *et al.*, Z. Phys. **C66**, 417 (1995).

[13] M. Aglietta *et al.*, Europhys. Lett. **8**, 611 (1989).

[14] T. Kafka, hep-ph/9712281.